Macromolecules

Volume 30, Number 8 April 21, 1997

Mechanism of Isoprene and Butadiene Polymerization in the Presence of $CpTiCl_3$−MAO Initiator: A Theoretical Study

Andrea Peluso,*,† Roberto Improta,‡ and Adolfo Zambelli†,§

Dipartimento di Chimica, Università di Salerno, via S. Allende, I-84081 Baronissi, Salerno, Italy, Cattedra di Chimica Teorica, Università Federico II, via Mezzocannone 4, I-80134 Napoli, Italy, and Dipartimento di Chimica Industriale, Politecnico di Milano, P.zza Leonardo da Vinci 32, I-20133 Milano, Italy

Received July 2, 1996; Revised Manuscript Received November 25, 1996[⊗]

ABSTRACT: The mechanism of butadiene and isoprene polymerization in the presence of $CpTiCl_3$ −MAO initiator has been investigated by means of EHT and *ab-initio* computations, with the purpose of understanding the factors responsible for the very different homopolymerization rates of the two monomers. The catalytically active species is assumed to be the highly unsaturated $[CpTi-R]^+$ organotitanium cation (R = growing polymer chain). It is shown that coordination of an incoming monomer to the active species forces the ending unit of R to rearrange from the initial η^3 allylic coordination to the σ one. This step is energetically much easier when the ending unit is butenyl rather than 2-methylbutenyl. No significant differences between butadiene and isoprene have been found for the insertion step; therefore, the large difference in the homopolymerization rates of butadiene and isoprene appears to be due to the highest reactivity of the growing chain ending with a butenyl unit.

Introduction

Among a number of homogeneous organometallic polymerization catalysts, $CpTiX_3$−MAO (Cp = Cyclopentadienyl; X = halide; MAO = methylaluminoxane) is particularly versatile and promotes polymerization of ethylene and α olefins,[1] conjugated diolefins,[2] styrene and substituted styrenes.[3] In the presence of this catalytic system, polymerization of conjugated diolefins and of styrenes is stereospecific, producing, e.g.,[1,4] cis polymers of 1,3-butadiene and isoprene[2] and 1,2-syndiotactic polymers of styrene and substituted styrenes[3] and of 4-methyl-1,3-pentadiene.[4] Substantial evidence has been reported in the literature, suggesting that the active species promoting polymerization of either conjugated diolefins or styrenes are $[CpTi-R]^+$ cations (R = growing polymer chain);[5,6] in addition, some crystalline cationic organometallic compounds have been reported,[7] which represent reasonable structural models for possibly intermediate species of the reaction mechanism. However, a detailed theoretical study of the polymerization mechanism is still lacking, although it would be useful for rationalizing the large amount of information and evidence experimentalists have deduced until now and hopefully for providing new hints and suggestions. As a first contribution, in this paper we report the results of a theoretical analysis whose main purpose is that of outlining the most important mechanistic aspects of the polymerization of conjugated diolefins in the presence of the $CpTiX_3$−MAO catalytic system.

The mechanism of Ziegler−Natta polymerization of conjugated diolefins has probably many common facets with that of monoalkenes. For the latter several reaction mechanisms have been proposed;[8−12] the most widely accepted mechanism is that proposed by Cossee and Arlman,[8] according to which the propagation of the polymer chain occurs in two steps. The first step involves the coordination of a monomer onto a vacant site of a metal complex with at least one alkyl ligand. Subsequently, the monomer inserts into the metal−alkyl σ bond, via a cyclic four-center transition state involving the alkyl group, the two unsaturated carbons of the monomer, and the transition metal. A slight modification of the Cossee−Arlman mechanism has been suggested by Brookhart and Green.[10−11] They pointed out that the insertion of the monomer into the metal−carbon bond can be assisted by agostic interactions between the unsaturated metal center and the α C−H bond of the growing polymer chain. Even in that case the insertion step proceeds via a metallacycle

† Università di Salerno.
‡ Università Federico II.
§ Politecnico di Milano.
⊗ Abstract published in *Advance ACS Abstracts,* February 1, 1997.

S0024-9297(96)00957-6 CCC: $14.00

Scheme 1

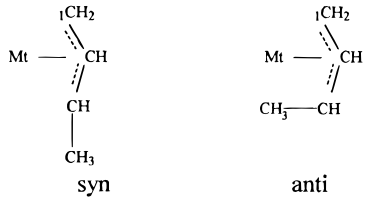

intermediate, followed by isomerization of the γ agostic intermediate to the product of the monomer insertion, restoring the initial α agostic interaction.

Several theoretical studies have been performed on simplified models of the catalytically active species, especially those derived by reacting a bis(cyclopentadienyl)titanium or -zirconium with a suitable cocatalyst.[13−23] Stationary points on the potential energy hypersurface associated with olefin coordination and insertion have been found,[14−16] confirming *grosso modo* the two-step mechanism. When the effects of dynamical correlation are taken into account, the region of the potential energy hypersurface corresponding to the coordination step appears to be very flat and that corresponding to the insertion step steeply descends from the coordination intermediate to the insertion products. As a result, no stationary points were found and the whole reaction appears to proceed downhill in energy.[17,19,20] However, experimental investigations would suggest a propagation barrier of 20−30 kJ/mol.[24,25] That discordance might be attributed either to the fact that computations on bare cationic species may underestimate both the coordination and the insertion barriers or to specific interactions of the active species with solvent molecules, usually aromatic species, which may be coordinated onto the vacant site of the active species, so that their displacement by the incoming monomer will require energy. Ziegler *et al.* have deeply investigated the role of agostic interactions using computations based on density functional theory (DFT) to account for the effects of dynamical correlation.[21,22] They have found that the agostic interaction of titanium with a β C−H is remarkably more stable than that with an α C−H and that the propagation barrier may be due to the isomerization from the β agostic to the α agostic complex, from which insertion occurs virtually without barrier.[22]

The polymerization of diolefins by Ziegler−Natta catalysts is also believed to be an insertion reaction,[2] but the polymerization mechanism is expected to be much more complicated than that of monoalkenes, as testified by the variety of structurally different products which can be obtained (see, *e.g.*, ref 2b and references therein). In fact, since the bond between the ending unit of the growing chain and the metal ion is expected to be of the π allylic type, different insertion pathways are possible. First, an allylic unit has two reactive sites, C_1 and C_3 (*cf.* Scheme 1), so that the products of both 1,2 and 1,4 polymerization can be obtained. Besides, the ending unit of the growing chain can be coordinated in two forms, the syn and the anti shown in Scheme 1, which give rise, in the case of 1,4 polymerization, to trans or cis polymers, respectively.

The syn form is expected to be thermodynamically the preferred one for butenyl groups not substituted at C_2,[26] but the anti form can be the predominant one for kinetic reasons, since, as generally accepted, it is formed by insertion of a monomer coordinated to a transition metal as a cis-η^4 ligand, a more stable coordination than the trans η^2 /η^4 one, whose insertion into the growing chain yields the syn form. The above considerations suggest that whenever the insertion step is fast enough to not allow for nuclear rearrangement, 1,4 cis polymers are obtained; on the contrary, if the monomer insertion is slow, as in 2,4-hexadiene, because of steric hindrances of the methyl groups, trans 1,4 polymers are obtained. Examples can be found in the literature where, depending on the substituents of the incoming monomer, on catalyst, and on polymerization conditions, both cis and trans polymers or a mixture of them can be obtained.[27]

Steric effects will also play a predominant role in determining whether the monomer insertion will occur at C_1 or C_3, but other factors are expected to be important, as suggested by the fact that polymerization of 1,3 pentadiene in the presence of $CpTiCl_3$ (Cp = cyclopentadienyl) activated by methylaluminoxane (MAO) yields the products of 1,2 polymerization at low temperature (253 K) and those of 1,4 polymerization at room temperature.[28]

Significant insight into the polymerization mechanism of conjugated olefins can be obtained by the analysis of homopolymerization and binary copolymerization rates and reactivity ratios.[29] The homopolymerization rates of the most common conjugated olefins have been studied using the $CpTiCl_3$−MAO catalyst. In comparable conditions, the homopolymerization rates increase in the following order:[30]

isoprene $\ll$ styrene $<$ butadiene $<$ 4-methyl-1,3-pentadiene

By definition, the homopolymerization rate of one particular monomer in the presence of a particular catalyst is the rate of incorporation of that monomer on one growing chain ending with the monomer unit resulting from the incorporation of that particular monomer, multiplied by the number of the growing chain ends. As a consequence, the values of homopolymerization rates jointly result from (i) the number of growing chain ends, (ii) the reactivity of the particular monomer, and (iii) the reactivity of the particular growing chain ends. A separate evaluation of the reactivities of different monomers and different growing chain ends can be obtained only by binary copolymerization experiments.[31] The evaluation of the reactivity ratios for butadiene−isoprene copolymerization has shown that butadiene and isoprene copolymerize almost at random and that the reactivities of the monomers in homopolymerizations do not parallel the relative reactivities in copolymerization.[30] The above finding is interesting and promises to be a relevant point for a better understanding of the mechanism of Ziegler−Natta polymerization of conjugated diolefins. In this paper some interesting results which can help identify the effects responsible of such observations are discussed.

Computational Details

The large size of the system under study and the necessity of testing several pathways and orientations have led us to start with the simple empirical EHT model,[32] using standard Hoffmann parameters.[33] Although EHT is a very simple method, unable to yield reliable total energies, it has been shown that, in the majority of the cases, it gives correctly both the shapes and the energy ordering of molecular orbitals (MO), thus being suitable to interpretative purposes, as testified by recent applications to mechanicistic aspects of Zie-

gler−Natta polymerizations of monoalkenes.[34] In order to have reasonable starting points for the structures of the active species and of some reaction intermediates, we have resorted to ab-initio UHF STO-3G computations. STO-3G is a minimal basis set, and therefore the accuracy of the results will be limited by the smallness of the basis set. A few computations using the split valence 3-21G basis set have been performed for the active species and for the most important reaction intermediate to test the accuracy of the results obtained using the minimal basis set. All *ab-initio* computations have been performed by the GAMESS package.[35]

Results

Active Species. Experimental evidence has suggested that the active species obtained by reacting $CpTiX_3$ with MAO is the organotitatium cation $[CpTi-R]^+$.[5,6] Thus, we have optimized at the *ab-initio* level, the structures of both the syn and the anti forms of $[CpTi-R]^+$, with R being a butenyl or 2-methylbutenyl unit (isoprene can give both the 2-methylbutenyl and the 3-methylbutenyl ending unit, but the former is expected to be the predominant one.[2b]) No constraints have been imposed in the optimization runs. The results of *ab-initio* optimizations are reported in Table 1, and the atom numbering is shown in Figure 1.

Ab-initio computations predict for either ending unit a π allylic coordination; the three unsaturated carbons of butenyl and 2-methylbutenyl are in fact at bonding distances from the titanium atom, and all interact with it. At the STO-3G level, the syn forms are predicted to be the electronically most stable ones for either ending unit. The differential energies are 8.9 and 7.6 kJ/mol for butenyl and 2-methylbutenyl, at the UHF level. However, the inclusion of electron correlation by the perturbative second-order Møller Plesset method (MP2), performed on the SCF optimized structures of the two forms, lowers the differential energy to 2.6 kJ/mol for butenyl and to 1 kJ/mol for 2-methylbutenyl. The same effect is also obtained by increasing the basis set; with the 3−21G basis set, the anti forms appear to be slightly more stable than the syn ones, even at the SCF level of theory; *cf.* Table 1. At any rate, the differential energies are very small, of the order of a thermal quantum (KT); therefore either form appears to be plausible and roughly equally probable. Thus, since no driving force for the syn−anti isomerization is predicted, the formation of cis or trans products will be essentially determined by the coordination mode of the monomer to the metal center, before insertion in the metal−carbon bond taking place.

Inspection of Table 1 shows that, at the STO-3G level, the butenyl and the 2-methylbutenyl groups are coordinated to the metal atom in quite different ways. Indeed, neither group exhibits an ideal allylic coordination mode, *e.g.* as occurs in the (η^3-allyl)(η^4-butadiene) Cp−Zr(II) complex,[36,37] where all three carbons of the allyl are at equal distances from the Zr ion (C_{allyl} −Zr ≈ 2.44 Å). In fact, in the active species, the Ti−C_1 and Ti−C_3 distances are shorter than the Ti−C_2 one, their STO-3G values being comparable with computed values for Ti−C σ bonds.[14,16,17] This is more evident for the butenyl ending unit in the syn form, whose coordination mode appears to be somewhat distorted toward a σ coordination. In fact, for the butenyl complex the Ti−C_1 bond distance is appreciably shorter than the Ti−C_3 one, whereas for the 2-methylbutenyl complex the above two distances are very similar. Significant differences are also found in the C−C bond distances of the two allyl units. For 2-methylbutenyl (syn form), the C_1-C_2 and C_2-C_3 bond distances are 1.46 and 1.42 Å, respectively, which are comparable with those of the allyl unit of the (η^3-allyl)(η^4-butadiene)Cp−Zr(II) complex, where $C_1-C_2 \approx C_2-C_3 \approx 1.44$ Å. For butenyl (syn form), the

Table 1. Selected Geometrical Parameters of the Optimized Structures of [CpTi−butenyl]$^+$ and [CpTi−2-methylbutenyl]$^+$ Complexes at the *ab-Initio* Level[a]

	syn		anti	
	STO-3G	3-21G[b]	STO-3G	3-21G[b]
	[CpTi−butenyl]$^+$			
C_1-Ti	2.05	2.20	2.09	2.24
C_2-Ti	2.34	2.38	2.30	2.36
C_3-Ti	2.28	2.36	2.24	2.31
C_4-Ti	3.53	3.54	2.70	2.71
$C_{Cp1}-Ti$	2.34	2.41	2.35	2.41
$C_{Cp2}-Ti$	2.32	2.39	2.31	2.40
$C_{Cp3}-Ti$	2.33	2.38	2.33	2.38
$C_{Cp4}-Ti$	2.32	2.40	2.33	2.39
$C_{Cp5}-Ti$	2.36	2.42	2.34	2.40
C_1-C_2	1.47	1.43	1.46	1.42
C_2-C_3	1.38	1.38	1.38	1.38
C_3-C_4	1.53	1.51	1.55	1.54
H_1-C_1	1.07	1.08	1.08	1.07
H_2-C_1	1.09	1.09	1.09	1.08
H_4-C_3	1.10	1.09	1.09	1.07
H_5-C_4	1.09	1.08	1.10	1.10
H_1-Ti	2.87	2.95	2.88	2.98
H_2-Ti	2.59	2.60	2.66	2.68
H_4-TI	2.45	2.53	3.07	3.08
H_5-Ti	3.75	3.72	2.37	2.35
$C_1-C_2-C_3$	116.5	119.7	117.5	120.2
$C_2-C_3-C_4$	123.9	124.2	121.5	121.2
$H_4-C_3-C_2$	113.7	115.6	118.1	119.2
$H_5-C_4-C_3$	110.8	116.2	116.3	116.0
$C_1-C_2-C_3-C_4$	175.1	174.0	−37.1	−29.3
$H_4-C_3-C_2-C_1$	38.4	30.4	7.5	7.7
E(SCF)	−1183.4016	−1189.9975	−1183.3982	−1189.9998
E(MP2)	−1183.9622	−1190.1786	−1183.9612	−1190.1811
E LUMO	−0.0410	−0.1155	−0.0343	−0.1084
ΔE_{coord}[c]	27.6	32.5	24.7	21.3
	[CpTi−2-methylbutenyl]$^+$			
C_1-Ti	2.09	2.23	2.12	2.24
C_2-Ti	2.36	2.41	2.33	2.37
C_3-Ti	2.15	2.28	2.15	2.28
C_4-Ti	3.45	3.46	2.69	2.69
$C_{Cp1}-Ti$	2.35	2.39	2.35	2.41
$C_{Cp2}-Ti$	2.35	2.40	2.31	2.40
$C_{Cp3}-Ti$	2.33	2.38	2.34	2.38
$C_{Cp4}-Ti$	2.34	2.39	2.34	2.40
$C_{Cp5}-Ti$	2.31	2.40	2.34	2.41
C_1-C_2	1.46	1.42	1.45	1.43
C_2-C_3	1.42	1.40	1.41	1.39
C_3-C_4	1.53	1.52	1.55	1.54
H_1-C_1	1.07	1.07	1.08	1.07
H_2-C_1	1.09	1.09	1.09	1.08
H_4-C_3	1.10	1.09	1.08	1.07
H_5-C_4	1.09	1.08	1.10	1.10
H_1-Ti	2.94	3.00	2.93	2.98
H_2-Ti	2.50	2.56	2.64	2.66
H_4-TI	2.45	2.48	2.99	3.05
H_5-Ti	3.63	3.68	2.41	2.33
$C_1-C_2-C_3$	112.6	116.3	113.8	117.6
$C_2-C_3-C_4$	121.2	119.2	121.5	121.3
$H_4-C_3-C_2$	108.9	114.1	118.0	118.8
$H_5-C_4-C_3$	110.7	112.0	116.3	116.2
$C_1-C_2-C_3-C_4$	175.6	175.6	−37.2	−48.1
$H_4-C_3-C_2-C_1$	51.7	36.9	7.5	6.9
E(SCF)	−1221.9925	−1128.8245	−1221.9896	−1228.8282
E(MP2)	−1222.6039		−1222.6035	
E LUMO	−0.0300	−0.1093	−0.0274	−0.1031

[a] Bond distances are in Å, angles in degrees, energies in atomic units, but for ΔE_{coord} which is in kJ/mol. The atom numbering is shown in Figure 1. [b] The MP2 computations with the 3-21G basis have been performed by omitting the highest 68 empty MOs. [c] ΔE_{coord} is the difference between the coordination energies of butenyl and 2-methylbutenyl.

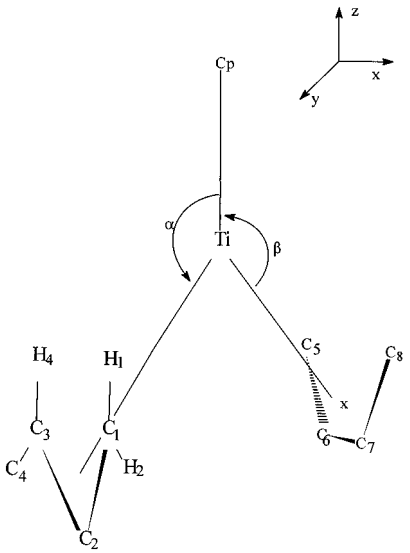

Figure 1. Adopted atom numbering.

C_1-C_2 bond distance is significantly longer than the C_2-C_3 one, values being 1.47 and 1.38 Å, respectively, as would be expected for a σ coordination mode. As a consequence, the 2-methylbutenyl unit is more strongly bound to $CpTi^{2+}$ than butenyl; at the UHF level, the coordination of 2-methylbutenyl is *ca.* 27 and 24 kJ/mol more exothermic than that of butenyl for the syn and anti forms, respectively. Another important difference between the [CpTi−butenyl]$^+$ and the [CpTi−2-methylbutenyl]$^+$ complexes is that the energy of the LUMO is lower for the former complex by *ca.* 28 and 18 kJ/mol for the syn and anti forms, respectively. This suggests that the active species with the polymer chain ending with a butenyl unit is a stronger electrophile than its counterpart with a 2-methylbutenyl ending unit.

The differences discussed above between the coordination modes of butenyl and 2-methylbutenyl are also found using the split valence 3-21G basis set (*cf.* Table 1). All the Ti−C bond distances slightly increase, so that the coordination modes of either butenyl and 2-methylbutenyl are less distorted with respect to those predicted by STO-3G computations. However, significant differences between the butenyl and 2-methylbutenyl coordination mode are still predicted (*cf.* Table 1). More importantly, the differences between the coordination energies of butenyl and 2-methylbutenyl to the $[CpTi]^{2+}$ unit and between the LUMO energies of the [CpTi−butenyl]$^+$ and [CpTi−2-methylbutenyl]$^+$ complexes, which are among the most important properties affecting the reactivity of the active species, are very similar to those predicted by STO-3G computations (*cf.* Table 1).

In order to better understand the factors responsible for those differences, which can play an important role in determining the very different homopolymerization rates of butadiene and isoprene, we have resorted to EHT computations. The interaction diagram for the syn coordination of butenyl and 2-methylbutenyl to the $[CpTi]^{2+}$ fragment is shown in Figure 2. The geometries adopted in the computations are those of Table 1 (STO-3G computations).

The interaction diagram for the coordination of either butenyl and 2-methylbutenyl fragments are very similar to each other, changing only for the energy of the MOs of the allylic unit. The $[CpTi]^{2+}$ fragment has four low lying empty MOs which can interact with the filled MOs of the allyl fragment. The most important interaction

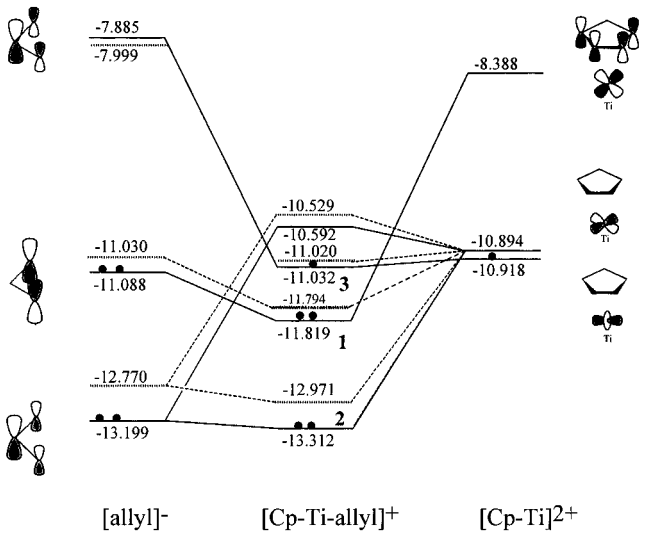

Figure 2. Most important electronic interactions for the coordination of an allyl unit to the $[CpTi]^{2+}$ fragment: (full lines) butenyl; (dashed lines) 2-methylbutenyl. Level energies are in eV. The empty MOs of the $[CpTi]^{2+}$ unit falling at −10.184 and −8.422 eV are not shown because they are not important for discussing the coordination step.

involves the HOMO of the allylic group and the third lowest unoccupied MO of the $[CpTi]^{2+}$ fragment, which is essentially given by the out of phase combination of a bonding π orbital of cyclopentadienyl with a d orbital (*i.e.* d_{xz} or d_{yz}, if the Cp plane is perpendicular to the *z* axis) of the metal cation, **1**. That interaction accounts for a large part of the coordination energy for either dienyl group, but the energy difference resulting from *ab-initio* computations between the coordination of 2-methylbutenyl and butenyl is due to the weak interaction of the HOMO-1 of the allylic group with the $d_{x^2-y^2}$ of $[CpTi]^{2+}$, **2**. In fact, the HOMO-1 of 2-methylbutenyl is at a higher energy than that of butenyl, for the weak antibonding interaction with orbitals of the methyl substituent; therefore its interaction with the empty $d_{x^2-y^2}$ of $[CpTi]^{2+}$ fragment is stronger. EHT computations predict for that interaction a stabilization energy of 0.20 eV *versus* 0.11 eV for butenyl, in line with *ab-initio* results. Finally, there is a weak interaction of back-donation between the singly occupied HOMO of $[CpTi]^{2+}$ and the LUMO of allyl, **3**.

For coordinating an incoming monomer, the [CpTi−allyl]$^+$ complexes, which *ab-initio* computations predict to have roughly a collinear configuration, have to relax toward a bent configuration. The allyl group can rotate about the metal center in two different ways, which gives rise to two different coordination modes: the endo one, with the central atom of allyl pointing toward the Cp ring or the exo one, with the open side of allyl oriented toward the Cp ring. The energies of the most important MOs as a function of the rotation angle are reported in Figure 3.

Figure 3 shows that a bent arrangement strongly stabilizes MO **1**. In fact, rotation of the allyl unit about the metal center brings the C_1 and C_3 carbons of the allyl close to the plane $z = 0$, namely the plane parallel to the Cp ring and containing the metal ion, so that the HOMO of allyl can now interact with the LUMO of the $CpTi^{2+}$ fragment (*cf.* Figure 2), being stabilized in energy. On the other hand, the bent configuration disfavors the singly occupied level **3**, since in such a configuration the interaction of the LUMO of the allyl fragment, which is mainly given by the C_2 π atomic

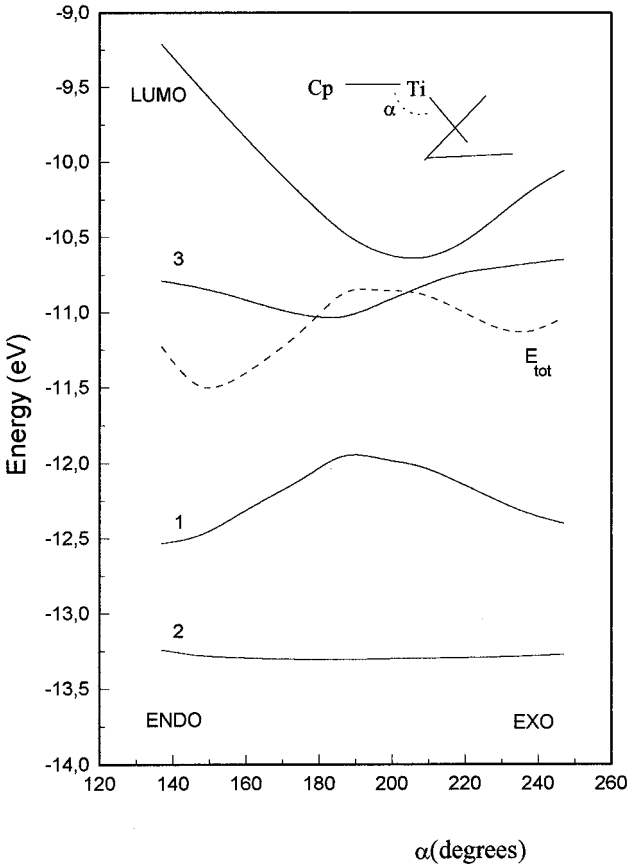

Figure 3. Energy variations of the most significant MOs of the $[CpTi-R]^+$ fragment as function of the allyl−Ti−Cp angle. The MO numbering is shown in Figure 2.

orbital, with the singly occupied $d_{x^2-y^2}$ of Ti is weakened, for the former is no longer pointing toward the $z = 0$ plane. On balance, considering the double occupancy of level **1**, either the endo or the exo arrangement appears to be preferred, at the EHT level, to the linear configuration predicted by *ab-initio* computations, as shown by the dashed line of Figure 3, representing the total energy of the system.

Both interactions **3** and **1** slightly favor the endo coordination of allyl with respect to the exo one. However, the LUMO of the latter is at a lower energy than that of the former and therefore an incoming monomer could be stronger coordinated when the allyl is in the exo form rather than in the endo one; thus both forms have to be considered in the analysis of the coordination step.

Coordination Step. Let us start by considering the rigid approach of cis butadiene in the exo arrangement to $[CpTi-butenyl]^+$, with the butenyl unit in the syn form and endo arrangement, the most stable form of the active species at the EHT level. The interaction diagram is shown in Figure 4.

There are two important interactions between the MOs of the $[CpTi-R]^+$ fragment and those of the incoming monomer: an attractive one, involving the HOMO of butadiene and the LUMO of $[CpTi-R]^+$, **4**, which is essentially an empty $d_{x^2-y^2}$ or d_{xy} orbital of the titanium ion, and a repulsive one which involves mainly the two occupied π MOs of the incoming monomer and the lowest occupied π MO of the ending unit of the growing chain, **5**, with a negligible contribution of d orbitals of the metal center. As the distance between the incoming monomer and the metal center decreases,

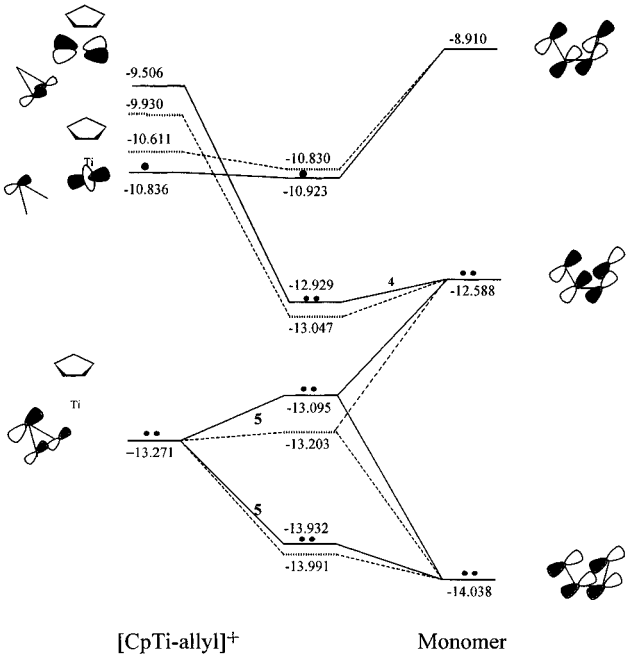

Figure 4. Most important electronic interactions for the coordination of butadiene to the $[CpTi-butenyl]^+$ fragment; (full lines) butenyl coordinated η^3 to Ti; (dashed lines) butenyl coordinated η^1 to Ti. Level energies in eV.

the energies of the two MOs involved in the repulsive interactions rise much more than the energy of the bonding MO lowers. As a result, the minimum energy configuration for the rigid approach of butadiene in the cis conformation occurs for $Ti-C_{monomer}$ distances of *ca.* 2.75 Å, in line with previous *ab-initio* computations for coordination of ethylene to bis(cyclopentadienyl)alkyltitaniums or zirconocenes.[16,17,20]

On changing the orientation of the ending unit of the growing chain from endo to exo, one finds only negligible variations in the interaction diagram. The attractive interaction **4** slightly enforces itself, because the LUMO of the $[TiCp-allyl]^+$ fragment is at a lower energy for the exo orientation of allyl, *cf.* Figure 3. However, the energy gain is modest and is balanced by the energy loss of MOs **3** and **1** of the $[CpTi-allyl]^+$ fragment. As concerns the incoming monomer, it contributes to both the attractive and repulsive interactions with both its inner and outer carbons; as a result the electronic energy is roughly independent on the relative orientation of the monomer with respect to the Cp ring. In conclusion, EHT computations suggest that there are no significant electronic effects discriminating between the endo and the exo orientations of both the allylic and the monomeric units, steric effects would play the predominant role in determining the most stable arrangement. A molecular mechanics study suggests that all the orientations are roughly at the same energy, but for the endo−endo one, whose energy is significantly higher.[38] However, as will be shown, the initial orientation of the ending unit of the growing chain has only a minor importance, since the coordination of butadiene or isoprene to the catalytically active species requires a substantial rearrangement of the allylic unit.

The repulsive interaction **5** is important, because, as for the insertion of ethylene into a M−H bond,[39] it could determine the reaction path for the coordination step. In fact, for the incoming monomer to approach the metal ion at distances short enough to allow its insertion into the Ti−allyl bond, the allyl ligand has to move from a

π to a σ coordination mode, so as to minimize the repulsion between the filled π orbitals of the ending unit of the growing chain and those of the incoming monomer. The interaction diagram of Figure 4 (dashed lines) shows that, on moving the allyl ligand toward a σ coordination mode, not only the repulsive interaction **5** is minimized but also the attractive interaction **4** becomes stronger, because the energy of the LUMO of the $[CpTi-R]^+$ unit diminishes, for the antibonding interaction between the C_3 of the allyl and the titanium ion is no longer present. *Ab-initio* STO-3G computations confirm the above finding, predicting that the energy of the LUMO diminishes by *ca.* 1 eV for the $\eta^3-\eta^1$ rearrangement of the allyl ligand. Moreover, the minimum energy configuration occurs now at a shorter Ti−monomer distance, the carbons of the incoming monomer being at 2.35−2.4 Å from the metal center.

The establishment of an equilibrium between the σ and π coordination modes of an allylic ligand upon coordination of a conjugated olefin is well-known in organometallic chemistry.[40−43] Detailed information on the insertion of butadiene into a metal−allyl bond has been provided by NMR measurements for the reaction of butadiene with $[(C_4H_7)PdCl_2]$.[42,43] In that case the reaction is slow enough to be followed by NMR. The results suggested that, upon coordination of one or more butadiene molecules, the C_4H_7 ligand, which was initially coordinated η^3 to Pd, moves toward a σ -η^1 coordination. Subsequently, butadiene inserts into the σ Pd−allyl bond and the π allylic coordination is restored. Thus, EHT computations suggest that a similar mechanism may be operative also in the case of the $CpTiX_3$−MAO initiator. This conjecture is important, because, as discussed in the previous section, the growing chain is stronger bound to the metal center when the ending unit is 2-methylbutenyl rather than butenyl; thus the transition from η^3 to η^1 is expected to be easier for butenyl than for 2-methylbutenyl. EHT estimates that, keeping fixed the position of the incoming monomer to that of the initial π complex, and rotating the allyl unit about the C_1 center, the $\eta^3 \rightarrow \eta^1$ rearrangement requires *ca.* 26 kJ/mol for butenyl and 41 kJ/mol for 2-methylbutenyl. This difference can be ascribed to a larger extent to the weakening of interaction **1**, because the contribution of the C_3 is higher for 2-methylbutenyl (20%) than for butenyl (12%).

To confirm the above scenario, we have resorted to *ab-initio* computations, optimizing the structures of $[CpTi(butenyl)(butadiene)]^+$ for both the syn and the anti forms of butenyl and for the syn form of $[CpTi(2\text{-methylbutenyl})(isoprene)]^+$ complexes. The results are reported in Table 2.

The conjecture that the coordination of a dienilic unit forces the growing chain to assume a σ coordination is confirmed by *ab-initio* optimizations. In fact, in all the complexes considered the η^3 coordination of allyl is strongly distorted: the distance C_1−Ti slightly decreases while the C_3−Ti one significantly increases, especially when butenyl is coordinated in the anti form, where it changes from 2.24 to 2.97 Å, according to the STO-3G computation, and from 2.31 to 2.78 Å, according to the 3-21G one. At any rate, the orientation of the C_2-C_3 double bond suggests that a weak interaction with the metal center is still present; this can be important in lowering the barrier for the insertion step. The geometry of the allyl unit also changes: the C_1-C_2 bond distance slightly increases, while the C_2-C_3 one decreases, and they assume values characteristic of a single and a double C−C bond, respectively. Thus, *ab-initio* computations suggest that already at the stage of monomer coordination, the allyl group assumes the geometry that it would have after the insertion reaction. As suggested in the literature,[2] the allyl coordinated in the syn form will yield trans products, whereas that coordinated in the anti form will yield cis products, as shown by the optimized values of the $\tau_{C_1-C_2-C_3--C_4}$ dihedral angle of Table 2.

Table 2. Selected Geometrical Parameters of the Optimized Structures of the $[CpTi(allyl)-monomer]^+$ Complexes at the *ab-Initio* STO-3G Level[a]

	I	II	III	
	STO-3G	STO-3G[b]	STO-3G	3-21G[b]
C_1-Ti	2.01	2.06	2.00	2.14
C_2-Ti	2.39	2.39	2.41	2.39
C_3-Ti	2.69	2.49	2.97	2.78
C_4-TI	3.91	3.74	3.54	3.41
C_5-Ti	2.75	2.44	2.83	2.91
C_6-Ti	2.66	3.01	2.60	2.64
C_7-Ti	3.09	3.69	2.81	2.69
C_8-Ti	3.73	4.24	3.70	3.13
$C_{Cp1}-Ti$	2.35	2.38	2.40	2.42
$C_{Cp2}-Ti$	2.33	2.36	2.38	2.44
$C_{Cp3}-Ti$	2.34	2.35	2.34	2.44
$C_{Cp4}-Ti$	2.38	2.35	2.37	2.43
$C_{Cp5}-Ti$	2.38	2.35	2.39	2.40
H_1-TI	2.76	2.81	2.70	2.82
H_2-TI	2.69	2.72	2.72	2.79
H_4-TI	2.83	2.58	3.73	3.46
C_1-C_2	1.50	1.50	1.51	1.48
C_2-C_3	1.36	1.37	1.36	1.35
C_3-C_4	1.52	1.52	1.52	1.52
C_5-C_6	1.34	1.37	1.33	1.33
C_6-C_7	1.50	1.50	1.51	1.49
C_7-C_8	1.32	1.32	1.34	1.33
H_1-C_1	1.08	1.08	1.08	1.08
H_2-C_1	1.09	1.08	1.08	1.08
H_4-C_3	1.09	1.09	1.09	1.07
$C_1-C_2-C_3$	121.6	116.3	126.2	125.4
$C_2-C_3-C_4$	123.9	126.3	127.2	126.3
$C_5-C_6-C_7$	126.9	123.6	125.2	126.6
$C_6-C_7-C_8$	125.4	124.5	126.7	125.7
$H_1-C_1-C_2$	110.9	109.2	109.5	113.7
$H_2-C_1-C_2$	110.0	111.6	110.6	115.7
$C_1-C_2-C_3-C_4$	175.1	178.0	17.8	25.3
$C_5-C_6-C_7-C_8$	14.0	28.3	15.3	9.4
E_{tot}(SCF)	−1336.4513	−1413.6294	−1336.4413	−1344.0798

[a] **I**, $[CpTi(butenyl)-butadiene]^+$ (syn form); **II**, $[CpTi(2\text{-methylbutenyl})-isoprene]^+$ (syn form); **III**, $[CpTi(butenyl)-butadiene]^+$ (anti form). Bond distances are in Å, angles in degrees, energies in atomic units; atom numbering is shown in Figure 1. [b] ROHF computation.

It is interesting to note that the coordination mode of monomer to Ti depends on the degree of $\eta^3 \rightarrow \eta^1$ rearrangement of the allyl ligand. The geometrical parameters of Table 2 suggest that for butenyl initially in the anti form, the case in which the transition to a σ coordination is more clearcut, butadiene appears to be coordinated η^3, whereas starting with butenyl in the syn form, the monomer is coordinated η^2. Finally, for the 2-methylbutenyl in the syn form only one carbon of the monomer is close to the metal center. These results further confirm that the electrophilicity of the $[CpTi-R]^+$ active species depends on the degree of distortion of the allyl coordination mode, increasing for increasing distortion toward a σ coordination.

Insertion Step. We start the analysis of the insertion step by localizing at the *ab-initio* level the transition state for the insertion of butadiene and isoprene into a $Ti-CH_3$ bond. The methyl group simulates the growing chain coordinated hapto1 to titanium. No constraints have been imposed. This step is necessary because for the insertion step several reaction paths could be

Table 3. Computed *ab-Initio* STO-3G Geometrical Parameters of Minimum Energy Configurations for Coordination of Butadiene and Isoprene to $[CpTi(CH_3)]^+$ and of Transition States for the Insertion Reactions[a]

	butadiene		isoprene	
	coordination	insertion	coordination	insertion
C_1-Ti	2.02	2.09	2.04	2.10
C_5-Ti	2.93	2.73	2.72	2.58
C_6-Ti	2.53	2.43	2.59	2.42
C_7-Ti	2.51	2.06	2.54	2.08
C_8-Ti	2.83	2.51	2.88	2.51
H_1-Ti	2.66	3.06	2.72	3.06
H_2-Ti	2.63	2.41	2.64	2.41
H_3-Ti	2.65	2.46	2.65	2.50
$C_{Cp1}-Ti$	2.33	2.35	2.36	2.36
$C_{Cp2}-Ti$	2.38	2.34	2.39	2.35
$C_{Cp3}-Ti$	2.36	2.35	2.35	2.34
$C_{Cp4}-Ti$	2.36	2.37	2.32	2.35
$C_{Cp5}-Ti$	2.36	2.39	2.34	2.39
C_5-C_6	1.34	1.36	1.34	1.36
C_6-C_7	1.50	1.48	1.51	1.48
C_7-C_8	1.34	1.41	1.34	1.41
C_1-C_8	3.98	2.19	3.40	2.19
H_1-C_1	1.08	1.07	1.08	1.07
H_2-C_1	1.08	1.09	1.08	1.09
H_3-C_1	1.08	1.09	1.08	1.09
$C_5-C_6-C_7$	126.0	123.3	122.7	119.6
$C_6-C_7-C_8$	126.1	119.4	126.5	119.9
$H_{12}-C_8-C_7$	123.0	121.3	123.2	121.4
$H_{13}-C_8-C_7$	120.6	118.6	120.3	118.5
$C_5-C_6-C_7-C_8$	5.2	25.9	14.1	30.2
$C_6-C_7-C_8-H_{12}$	5.6	16.1	3.2	16.5
$C_6-C_7-C_8-H_{13}$	−0.3	−11.8	−1.4	−10.2
E_{tot}(SCF)	−1222.9230	−1222.8826	−1260.5108	−1260.4691
E_{tot}(MP2)	−1223.5519	−1223.5118	−1261.1928	−1261.1549

[a] Bond distances are in Å, angles in degrees, energies in atomic units; for the atom numbering see Figure 1.

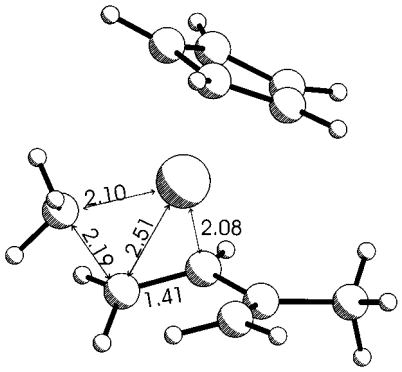

Figure 5. *Ab-initio* optimized structures of the saddle point for insertion of 2-methylbutenyl into the $Ti-CH_3$ bond. Distances in Å.

possible. Thus, we will use the structure obtained by the *ab-initio* saddle point computation on the model system as the starting point for the EHT analysis of the orbital evolution in the insertion step. An accurate evaluation of the barrier for the insertion step at the *ab-initio* level is not possible at this stage, both because the substitution of the allyl unit with a methyl is expected to increase the activation energies, for the stabilizing effect of the coordination of the C−C double bond of the ending unit of the growing chain to titanium is lost, and because of the small size of the basis set and the neglect of the effects of dynamical correlation.

The results of *ab-initio* computations, reported in Table 3 and Figure 5, show that in the saddle points either monomer is coordinated to Ti with one of the two inner carbons, that bound to the carbon which will insert in the $Ti-CH_3$ bond, much close to the metal center of all the others. The relative C=C double bonds are lengthened from 1.34 to 1.41 Å for either butadiene or isoprene. The methyl group forms two agostic interactions with Ti, as shown by the slight lengthening of two C−H bond distances. The distance between the two carbons which have to form the new C−C bond is 2.2 Å, in line with previous accurate *ab-initio* computations for polymerization of monoalkenes with bis(cyclopentadienyl)titanium.

The geometries of Table 3 have been adopted as a starting point for the EHT analysis of the orbital evolution from the minimum energy configurations of the coordination steps to the activated states of the insertion step. The butenyl and 2-methylbutenyl unit have been restored in place of the methyl one, starting with the $Ti-C_1$ distance predicted by the *ab-initio* computation for the $Ti-CH_3$ bond in the saddle points and orienting the rest of the chain in such a way to have the best interaction of the π orbitals with the d orbitals of the metal.

EHT computations show that there are no significant repulsive interactions between the orbitals of the allyl unit and those of the incoming monomer, in particular between those of the two carbons which have to form the new C−C bond. This is possible because of the HOMO−LUMO mixing occurring in the diene moiety. The role of the LUMO is similar to that discussed by Thorn and Hoffmann for the insertion of ethylene into a Pd−H bond,[39] it cancels the contribution to the HOMO of the monomer carbon which has to interact with the ending carbon of the growing chain, reducing the barrier for the formation of the new C−C bond. Thus, the barrier for the insertion reaction is mainly due to the geometrical distortion of the incoming monomer in the activated state, since the HOMO−LUMO mixing causes a significant lengthening of the C=C double bonds, especially that involved in the formation of the new C−C bond and a slight shortening of the C−C single bond; *cf.* Table 3. EHT predicts that this distortion requires *ca.* 66 and 71 kJ/mol for the insertion of butadiene and isoprene into the $Ti-CH_3$ bond, respectively. However, these activation energies are lowered by the interaction of the C=C double bond of the ending unit of the growing chain with the metal center which is much stronger in the activated state than in the coordination intermediate. On balance, the activation energies for the insertion of butadiene and isoprene into the Ti−butenyl and Ti−(2-methylbutenyl) bond are predicted to be *ca.* 9 and 11 kJ/mol, respectively.

The results of the EHT analysis give two important hints: (i) the barrier for the insertion step is predicted to be low, in line with the theoretical data reported in the literature for the insertion of ethylene in a Ti−C bond;[19−22] (ii) no relevant differences for the insertion of butadiene into a Ti−butenyl bond and that of isoprene into a Ti−2-methylbutenyl bond have been found, confirming that the rate-determining step of homopolymerizations must be the coordination of the monomer to the active catalytic species. Indeed, only for that step have we found significantly different activation energies between butadiene and isoprene.

Summary and Conclusion

The EHT analysis of the homopolymerization mechanism of butadiene and isoprene with $TiCl_3$−MAO catalyst suggests that the mechanism of the propagation reaction can be divided into two steps: a rate-determining step consisting of the coordination of monomer to the active catalytic species and a faster step involving the insertion of the incoming monomer into the growing

polymer chain. The monomer coordination step requires a substantial rearrangement of the ending unit of the growing polymer chain from the η^3 coordination to the η^1 one. That rearrangement is important because it minimizes the repulsive interactions between the π orbitals of the ending unit of the growing polymer chain and those of the incoming monomer and it lowers the energy of the LUMO of the active catalytic species $[CpTi-allyl]^+$ which is involved in the bonding interaction with the π orbitals of the incoming monomer. Both effects allow the incoming monomer to approach the metal center at distances short enough for the insertion into the Ti−allyl bond can take place. The location of a few stationary points on the potential energy hypersurface performed at *ab-initio* level with a minimal basis set has confirmed the above conjecture: the minimum energy configurations for the products of the coordination steps are those with allyls coordinated η^1 to the metal center, either for butadiene inserting into the Ti−butenyl bond and for isoprene inserting into the Ti−2-methylbutenyl bond. The accuracy of these results is limited by the smallness of the basis set employed here and will require further refinements; a test computation with a larger 3-21G basis for the [Cp−Ti(butenyl)-(butadiene)]$^+$ has confirmed the STO-3G results.

According to EHT computations, the $\eta^3-\eta^1$ rearrangement requires activation energies of *ca.* 26 kJ/mol for butenyl and 41 kJ/mol for 2-methylbutenyl. On the other hand, no significant differences between the two monomers have been found for the insertion step. A high barrier is predicted by both EHT and *ab-initio* computations for either monomer inserting into the Ti−methyl bond, with the methyl group simulating the ending unit of the growing polymer chain, which is coordinated η^1 to the metal center. However, the EHT analysis suggests that the back-biting of the C=C double bond to titanium can significantly lower the barrier to *ca.* 9 kJ/mol for the insertion of butadiene into the Ti−butenyl bond and to 11 kJ/mol for the insertion of isoprene into the Ti−2-methylbutenyl bond.

The above activation energies must be taken as qualitative indications, since they have been obtained by an approximate method such as the EHT, with an approximate location of the saddle points. In fact, since an automatic location of the saddle point is not possible at the EHT level, one step could be accidentally treated better than the other. With this warning in mind, we observe that EHT barriers are able to explain the observed trend of homopolymerization rates: the higher homopolymerization rate of butadiene with respect to isoprene is ascribed to the lower reactivity of the growing chain ending with a 2-methylbutenyl unit; the latter exhibits an almost ideal η^3 coordination in the active species and is more strongly bound to the metal center than the butenyl ending unit, whose coordination mode is somewhat distorted toward a σ coordination. A thorough understanding of the relative reactivities observed in copolymerization experiments will require the evaluation of the reactivity of each monomeric unit for each active species ending with either allyl group; work on this line is actually in progress. However, the above results are sufficient to explain why, despite the large difference between butadiene and isoprene homopolymerization rates (2−3 orders of magnitude[30a]), the reactivity ratios for butadiene−isoprene copolymerization are of the order of unity. The reactivity ratio, $r_{ij} = K_{ii}/K_{ij}$, is the ratio of the rates of insertion of two different monomers M_i and M_j into the Ti−R_i bond, R_i being the ending unit of the growing polymer chain derived by the insertion of M_i and K_{ij} being the rate for the reaction:

$$CpTi-M_i + M_j \rightarrow CpTiM_j-M_i$$

If our conjecture holds, the value of K_{ij} will depend mainly on M_i and much less on M_j and, therefore, the reactivity ratios for isoprene−butadiene copolymerization will be of the order of unity, as observed.

As concerns the site of attack, our computations predict that the C_1 site is the preferred one for either monomer, in line with experimental findings that both isoprene and butadiene yield the products of 1,4 polymerization. The computed transition state for the insertion of isoprene into the Ti−CH_3 bond (*cf.* Figure 5) confirms the expectation[2b] that isoprene gives preferentially the 2-methylbutenyl derivative instead of the 3-methylbutenyl one. Finally, the earlier suggestion that the stereospecificity of the polymer products depends on the initial coordination form of the allyl unit, namely that allyls coordinated in the syn form will yield trans products whereas those coordinated in the anti form will yield cis products,[2] is confirmed by the results of *ab-initio* optimizations.

Acknowledgment. The financial support of MURST and CNR (Italy) is gratefully acknowledged.

References and Notes

(1) Kaminski, W.; Min, M.; Sinn, H.; Woldt, R. *Makromol. Chem., Rapid. Commun.* **1983**, *4*, 417.
(2) (a) Porri, L.; Giarrusso, A.; Ricci, G. *Prog. Polym. Sci.* **1991**, *16*, 405. (b) Porri, L.; Giarrusso, A. Conjugated diene polymerization; *Comprehensive Polymer Science*; Eastmond, G. C., Ledwith, A., Russo, S., Sigwalt, P., Eds.; Pergamon Press: Oxford, U.K., 1989; Vol. 4, Part II, pp 53−108. (c) Oliva, L.; Longo, P.; Grassi, A.; Ammendola, P.; Pellecchia, C. *Makromol. Chem., Rapid Commun.* **1990**, *11*, 519.
(3) (a) Ishihara, N.; Kuramoto, M.; Uoi, M. *Macromolecules* **1988**, *21*, 3356. (b) Zambelli, A.; Oliva, L.; Pellecchia, C. *Macromolecules* **1989**, *22*, 2129.
(4) (a) Zambelli, A.; Ammendola, P.; Proto, A. *Macromolecules* **1989**, *22*, 2186. (b) Porri, L.; Galeazzi, M. C. *Eur.* Polym. J. **1966**, *2*, 189.
(5) Zambelli, A.; Pellecchia, C.; Oliva, L.; Longo, P.; Grassi, A. *Makromol. Chem.* **1991**, *192*, 223.
(6) Pellecchia, C.; Longo, P.; Proto, A.; Zambelli, A. *Makromol. Chem., Rapid. Commun.* **1992**, *13*, 265.
(7) (a) Pellecchia, C.; Immirzi, A.; Pappalardo, D.; Peluso, A. *Organometallics* **1994**, *13*, 3773. (b) Pellecchia, C.; Grassi, A.; Immirzi, A. *J. Am. Chem. Soc.* **1993**, *115*, 1160.
(8) (a) Cossee, P. *J. Catal.* **1964**, *3*, 80. (b) Arlman, E. J.; Cossee, P. *J. Catal.* **1964**, *3*, 99.
(9) Ivin, K. J.; Rooney, J. J.; Stewart, C. D.; Green, M. L. H.; Mahtab, R. *J. Chem. Soc., Chem. Commun.* **1978**, 604.
(10) Brookhart, M.; Green, M. L. H.; Pardy, R. B. A. *J. Chem. Soc., Chem.* Commun. **1983**, 691.
(11) Brookhart, M.; Green, M. L. H. *J. Organomet. Chem.* **1983**, *250*, 395.
(12) Istenes, M. *J. Catal.* **1991**, *129*, 383.
(13) Fujimoto, H.; Yamasaki, T.; Mizutani, H.; Koga, N. *J. Am. Chem. Soc.* **1985**, *107*, 6157.
(14) Kawamura-Kuribayashi, H.; Koga, N.; Morokuma, K. *J. Am. Chem. Soc.* **1992**, *114*, 2359, 8687.
(15) Castonguay, L. A.; Rappé, A. K. *J. Am. Chem. Soc.* **1992**, *114*, 5832.
(16) Sakay, S. J. *J. Phys. Chem.* **1994**, *98*, 12053.
(17) Weiss, H.; Ehrig, M.; Ahlrichs, R. *J. Am. Chem. Soc.* **1994**, *116*, 4919.
(18) Bierwagen, E. P.; Bercaw, J. C.; Goddard, W. A., III. *J. Am. Chem. Soc.* **1994**, *116*, 1481.
(19) Meier, R. J.; van Doremaele, G. H. J.; Iarlori, S.; Buda, F. *J. Am. Chem. Soc.* **1994**, *116*, 7274.
(20) Jensen, V. R.; Børve, K. J.; Ystenes, M. *J. Am. Chem.* Soc. **1995**, *117*, 4109.

(21) Woo, T. K.; Fan, L.; Ziegler, T. *Organometallics* **1994**, *13*, 2252.
(22) (a) Lohrenz, J. C. W.; Woo, T. K.; Ziegler, T. *J. Am. Chem. Soc.* **1995**, *117*, 12793. (b) Margl, P.; Lohrenz, J. C. W.; Ziegler, T.; Blöchl, P. E. *J. Am. Chem. Soc.* **1996**, *118*, 4434.
(23) Siegbhan, P. E. M. *Chem. Phys. Lett.* **1993**, *205*, 290.
(24) Natta, G.; Zambelli, A.; Pasquon, I.; Giongo, G. M. *Chim. Ind.* **1966**, *48*, 1298.
(25) (a) Chien, J. C. W.; Razavi, A. *J. Polym. Sci., Part A: Polym.* Chem. **1988**, *26*, 2369. (b) Chien, J. C. W.; Sugimoto, R. *J. Polym. Sci., Part A: Polym.* Chem. **1991**, *29*, 459. (c) Chien, J. C. W.; Bor-Ping Wang, J. *J. Polym. Sci., Part A: Polym. Chem.* **1990**, *28*, 15.
(26) (a) Druz, N. N.; Zak, A. V.; Lobach, M. I.; Shpakov, P. P.; Kormer, V. A. *Eur. Polym. J.* **1977**, *13*, 875. (b) Taube, R.; Gehrke, J. P.; Schmidt, U. *Makromol. Chem. Macromol.* Symp. **1986**, *3*, 389.
(27) Natta, G.; Porri, L.; Carbonaro, A. *Makromol. Chem.* **1964**, *77*, 26. Natta, G.; Porri, L.; Carbonaro, A.; Stoppa, G. *Makromol. Chem.* **1964**, *77*, 114. See also ref 2b and references therein.
(28) Ricci, G.; Italia, S.; Porri, L. *Macromolecules* **1994**, *27*, 868.
(29) (a) Kormer, V. A.; Lobach, M. I.; Klepikova, V. I.; Babitskii, B. D. *Polym. Lett. Ed.* **1976**, *14*, 317. (b) Warin, R.; Julemont, M.; Teyssié, Ph. *J. Organomet. Chem.* **1980**, *185*, 413. (c) Sokolov, V. N.; Khvostic, G. M.; Poddumnyi, I. Ya.; Kondratenkov, G. P. *J. Organomet. Chem.* **1971**, *29*, 313.
(30) (a) Zambelli, A.; Proto, A.; Longo, P.; Oliva, P. *Macromol. Chem. Phys. 195*, 2623, **1994** and references therein; Pellecchia, C.; Proto, A.; Zambelli, A. *Macromolecules* **1992**, *25*, 4450.
(31) (a) Copolymerizations; Ham, G. E., Ed.; Interscience Publishers: New York, 1964. (b) Mayo, F. R.; Walling, C.; Lewis, F. M.; Hulse, W. F. *J. Am. Chem. Soc.* **1948**, *70*, 1523.
(32) (a) Hoffmann, R.; Lipscomb, W. N. *J. Chem. Phys.* **1962**, *36*, 3179, 3489. (b) Hoffmann, R. *J. Chem. Phys.* **1963**, *65*, 1397.
(33) Lauher, J. W.; Hoffmann, R. *J. Am. Chem. Soc.* **1976**, *98*, 1729.
(34) (a) Prosenc, M. H.; Janiak, C.; Brintzinger, H. H. *Organometallics* **1992**, *11*, 4036. (b) Janiak, C. *J. Organomet.* Chem. **1993**, *452*, 63. (c) Mohr, R.; Berke, H.; Erker, G. *Helv.* Chim. Acta **1993**, *76*, 1389. (d) Gleiter, R.; Hyla-Kryspin, I.; Niu, S.; Erker, G. *Organometallics* **1993**, *12*, 3828.
(35) (a) Guest, M. F.; Sherwood, P. GAMESS, an *ab initio* program. The Daresbury Laboratory: Warrington, U.K. (b) Schmidt, M. W.; Baldridge, K. K.; Boatz, J. A.; Elbert, S. T.; Gordon, M. S.; Jensen, J. J.; Koseki, S.; Matsunaga, M.; Nguyen, K. A.; Su, S.; Windus, T. L.; Dupuis, M.; Montgomery, J. A. *J. Comput. Chem.* **1993**, *14*, 1347.
(36) Erker, G.; Berg, K.; Krüger, C.; Müller, G.; Angermund, K.; Benn, R.; Schroth, G. *Angew. Chem., Int. Ed. Engl.* **1984**, *23c*, 455.
(37) Erker, G. *J. Organomet. Chem.* **1990**, *400*, 185.
(38) Guerra, G.; Cavallo, L.; Corradini, P.; Fusco R. *Macromolecules*, submitted for publication.
(39) Thorn, D. L.; Hoffmann, R. *J. Am. Chem. Soc.* **1978**, *100*, 2079.
(40) Lukas, J.; Van Leeuwen, P. W. N. M.; Volger, H. C.; Kouwenhoven, A. P. *J. Organomet. Chem.* **1973**, *47*, 153.
(41) Van Leeuwen, P. W. N. M.; Praat, A. *J. Organomet. Chem.* **1970**, *21*, 501.
(42) Powell, J. *J. Chem. Soc. A* **1971**, 2233.
(43) Hughes, R. P.; Powell, J. *J. Am. Chem. Soc.* **1972**, *94*, 7723.

MA960957F